Biology of Reproduction, 2021, 104(1), 197–210
doi:10.1093/biolre/ioaa191
Research Article
Advance Access Publication Date: 13 October 2020

OXFORD

Research Article

Maternal obesity alters placental lysophosphatidylcholines, lipid storage, and the expression of genes associated with lipid metabolism‡

Katie L. Bidne[1,†], Alana L. Rister[2,†], Andrea R. McCain[1], Brianna D. Hitt[3], Eric D. Dodds[2,4] and Jennifer R. Wood[1,*]

[1]Department of Animal Science, University of Nebraska-Lincoln, Lincoln, NE, USA, [2]Department of Chemistry, University of Nebraska-Lincoln, Lincoln, NE, USA, [3]Department of Statistics, University of Nebraska-Lincoln, Lincoln, NE, USA and [4]Nebraska Center for Integrated Biomolecular Communication, University of Nebraska-Lincoln, Lincoln, NE, USA

*__Correspondence__: Department of Animal Science, University of Nebraska-Lincoln, 3940 Fair St., Lincoln, NE 68583-0908, USA. Tel: 1-402-472-6437; E-mail: jwood5@unl.edu

†These authors contributed equally to this work.

‡This study was supported by funds from NIFA Research Capacity Funding (USDA 1013511), University of Nebraska Foundation, Nebraska Center for Integrated Biomolecular Communication (NIH P20GM113126) and Molecular Mechanisms of Disease Predoctoral Training Program (NIH T32GM107001), NE-INBRE (P20GM103427-14), CoBRE (P30GM110768), Fred & Pamela Buffett Cancer Center (P30CA036727), Center for Root and Rhizobiome Innovation (36-5150-1085-20) and the Nebraska Research Initiative.

Conference Presentation: Presented in part at the Perinatal Biology Symposium, 24–27 August 2019, Snowmass, Colorado, and the American Society for Mass Spectrometry Asilomar Conference, 11–15 October 2019, Pacific Grove, CA., and the Society for the Study of Reproduction Virtual Annual Meeting, 8–12 July 2020.

Received 12 May 2020; Revised 21 September 2020; Editorial Decision 8 October 2020; Accepted 9 October 2020

Abstract

Dyslipidemia is a characteristic of maternal obesity and previous studies have demonstrated abnormalities in fatty acid oxidation and storage in term placentas. However, there is little information about the effect of pre-pregnancy obesity on placental lipid metabolism during early pregnancy. The objective of this study was to determine the relationship between lipid profiles and markers of metabolism in placentas from obese and lean dams at midgestation. Mice were fed a western diet (WD) or normal diet (ND) and lysophosphatidylcholines (LPCs) and/or phosphatidylcholines (PCs) were measured in dam circulation and placenta sections using liquid chromatography–tandem mass spectrometry and mass spectrometry imaging, respectively. In WD dam, circulating LPCs containing 16:1, 18:1, 20:0, and 20:3 fatty acids were increased and 18:2 and 20:4 were decreased. In WD placenta from both sexes, LPC 18:1 and PC 36:1 and 38:3 were increased. Furthermore, there were moderate to strong correlations between LPC 18:1, PC 36:1, and PC 38:3. Treatment-, spatial-, and sex-dependent differences in LPC 20:1 and 20:3 were also detected. To identify genes that may regulate diet-dependent differences in placenta lipid profiles, the expression of genes associated with lipid metabolism and nutrient transport was measured in whole placenta and isolated labyrinth using droplet digital PCR and Nanostring nCounter assays. Several apolipoproteins were increased in WD placentas. However, no differences in nutrient

transport or fatty acid metabolism were detected. Together, these data indicate that lipid storage is increased in midgestation WD placentas, which may lead to lipotoxicity, altered lipid metabolism and transport to the fetus later in gestation.

Summary sentence

At midgestation, lipid profiles are altered in the circulation of obese mouse dams and placentas with specific changes in phosphatidylcholine and lyso-phosphatidylcholine species, lipid storage, and the expression of apolipoproteins.

Graphical Abstract

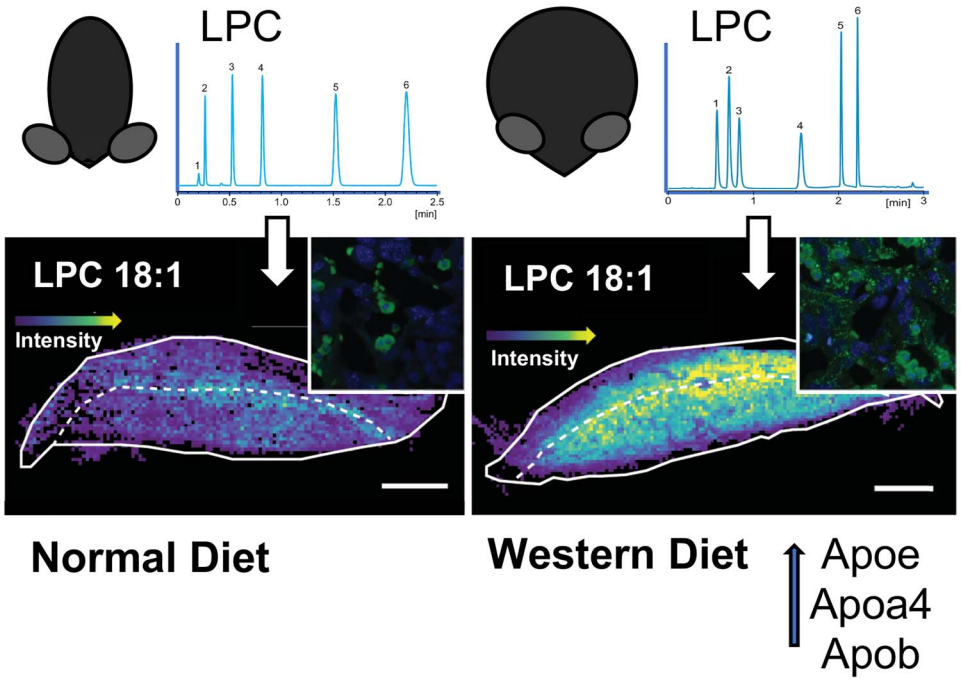

Key words: placenta, pregnancy, metabolism, nutrition, developmental biology.

Introduction

Approximately one-third of reproductive-aged women in the USA are classified as obese [1] with even higher rates in Hispanic (51%) and African–American (55%) populations. Elevated maternal body mass index is associated with increased birthweight and adipose tissue accumulation in infants [2, 3] which increases offspring risk of developing metabolic disease later in life [4]. The placenta is a transient but essential organ that regulates nutrient transport between maternal and fetal circulations [5–7]. Therefore, it is no surprise that placenta function is a major determinant of fetal growth and mediates, in part, the effects of maternal obesity on negative fetal outcomes.

The placenta has a high metabolic rate [8]. Therefore, maternal nutrients are not only transferred to the fetus but also used to meet the energy requirements of the placenta. Both glucose and fatty acid are taken up by placental syncytiotrophoblasts and subsequently undergo oxidative phosphorylation and β-oxidation, respectively in cytotrophoblasts to generate ATP [9, 10]. Mild hyperlipidemia is a characteristic of normal pregnancy. Hyperlipidemia is also a common phenotype of obesity. Therefore, obese women typically exhibit moderate to severe increases in circulating fatty acids which leads to increased fatty acid β-oxidation [10] and lipid accumulation in the placenta [11, 12]. This creates a lipotoxic environment that is associated with increased inflammation, oxidative stress, and impaired placental function [8, 13].

Most fatty acids circulate in lipoprotein complexes which include phospholipids, triglycerides, and cholesterol. Phosphatidylcholines (PC) are one of the phospholipid species in circulating lipoproteins. They are also the major component of plasma and organelle membranes including lipid droplets, which are the storage site of fatty acids within a cell [14, 15]. PCs contain a phosphocholine headgroup and two fatty acid tails. De novo synthesis is regulated by enzymes of the Kennedy cycle (CEPT, PCYT1A) [16]. Alternatively, PC is generated by methylation of phosphatidylethanolamine by PE methyltransferase (PEMT) enzymes [16]. PCs are metabolized via the Lands' cycle into one-tailed lysophosphatidylcholine (LPC) by phospholipases [17]. The addition of a fatty acid tail to LPCs, which regenerates PCs, is regulated by lysophophatidylcholine acyltransferase (LPCAT) [18]. Importantly, LPC species are generally proinflammatory due to activation of signaling pathways which subsequently induce cytokine production [19–22].

Regulation of lipid metabolism in the placenta has been primarily studied using primary human trophoblast cells collected after parturition (vaginal delivery or cesarean section) from lean

or obese women. Human and mouse placentas are structurally and functionally similar [23]. Therefore, studies using mouse models of obesity and/or gestational diabetes have also been performed using placentas collected at the end of gestation. However, little is known about the effects of maternal dyslipidemia during development of the placenta. In the mouse, the placenta reaches functional and structural maturity around midgestation (~embryonic day 10.5–12.5), which corresponds to the beginning of the 2nd trimester of a human pregnancy [24, 25]. Recent transcriptomics data also show enrichment of genes associated with lipid transport and metabolism in the embryonic day 12.5 (E12.5) placenta [26]. Therefore, in this study, we utilized a mouse model of maternal obesity to test our hypothesis that diet-induced obese dams have increased circulating lipids at E12.5 resulting in altered lipid metabolism and storage in the placenta.

Materials and methods

Animals and animal care

All animal experiments were approved by the University of Nebraska-Lincoln Institutional Animal Care and Use Committee.

C57BL/6J (B6) females were randomly assigned to western-style diet (WD, Envigo TD.88137) or normal rodent chow (ND, Teklad Global 18% protein rodent diet) experimental groups. Normal rodent chow is 14.3% crude protein, 48% carbohydrate (ground corn and corn gluten meal), and 4% fat. The fat was 0.6% saturated, 0.7% monounsaturated, and 2.1% polyunsaturated. The major fatty acid was linoleic (18:2 n6, 2%) followed by oleic (18:1 n9, 0.7%), palmitic (16:0, 0.5%), stearic (18:0, 0.1%), and linolenic (18:3 n3, 0.1%). There was no cholesterol in the normal rodent chow. The western-style diet was 17% protein, 48.5% carbohydrate (34% sucrose), and 21% fat. The fat was 12.8% saturated, 5.6% monounsaturated, and 1% polyunsaturated. Cholesterol (0.2%) was also included in the diet. The major fatty acid was palmitic (5.8%) followed by oleic (4.2%), stearic (2.5%), linoleic (0.5%), and linolenic (0.2%).

Mice were maintained on their respective diets for 10–12 weeks. All animals had ad libitum access to food and water and were maintained on a 12:12 light:dark cycle. WD and age-matched controls were bred to B6 control males and checked for a vaginal plug to confirm pregnancy. Dietary treatments (ND or WD) were maintained during pregnancy. Dams were euthanized at E12.5 of pregnancy using isoflurane overdose and exsanguination.

Tissue collection and processing

Dam blood was collected by cardiac puncture. Whole blood was incubated on ice for 2 h and room temperature for 1 h prior to centrifugation at 900 rcf for 18 min. Resulting serum was stored at −80°C. Dam adipose was excised and weighed. Dam liver was excised and fixed using 4% paraformaldehyde (PFA) overnight at 4°C. Each pregnant uterus was removed and dissected to collect individual fetuses and placentas. Fetal and placental weight were recorded, and whole placenta fixed in 4% PFA overnight at 4°C. Fetal tails were snap frozen and stored at −20°C. Fixed tissues were incubated in 30% sucrose overnight followed by an overnight incubation in 50:50 solution of 30% sucrose and 30% OCT (Fisher Healthcare 4585). Tissues were embedded in OCT and stored at −20°C. Placenta labyrinth was isolated by microdissection from a subset of placentas as previously described [27]. Briefly, uterine muscle was removed from an individual implantation site to expose the placenta. Decidua was separated and junctional layer was trimmed away from the labyrinth under a dissection microscope. Labyrinth was weighed, flash frozen, and stored at −80°C.

DNA extraction and genotyping

DNA was extracted from fetal tails using 500 µL tail buffer (Teknova T0525) containing 14.6 µL proteinase K (New England Biolabs P8107S). Samples were incubated overnight in 55°C water bath and precipitated using 140 µL 6 M NaCl. DNA pellet was washed with 70% ethanol, air dried, and resuspended in 20 µL of Millipore water and stored at −20°C. Polymerase chain reaction (PCR) master mix was made by adding one Illustra PuReTaq Ready-To-Go PCR bead (GE Healthcare 27-9559-01) to 23 µL of ddH_2O. One microliter of DNA was added and 10 µM of primers for SRY (IDT F-CGCCATCCATGTCAAGCGCCCCATGA, R-GCGGAATTCACTTTAGCCCTCCGATG). Twenty-nine cycles of PCR were performed as follows: (1) 94°C for 1 min, (2) 58°C for 1 min, (3) 72°C for 1 min. The reaction was subsequently incubated at 72°C for 5 min. Six microliters of PCR product was run on a 1% agarose gel and imaged. Samples positive for *Sry* were identified as male whereas samples negative for *Sry* were identified as female.

Liver and placenta BODIPY staining

Serial transverse sections (10 µm) of cryopreserved dam livers and placentas were adhered to slides. Slides were dried at 37°C for 45 min, rinsed twice in Phosphate buffered saline (PBS) with (liver) or without (placenta) 1.5 mg/mL glycine for 10 min, and stained with 1:5000 (liver) or 1:1000 (placenta) dilution of BODIPY 493/503 (Thermofisher D3922) in PBS for 20 min. Slides were rinsed three times in PBS for 5 min, then stained with DAPI nuclear marker at a 1:1000 dilution for 4 min. Slides were washed in ddH_2O for 5 min and mounted using Prolong Gold (Invitrogen P36934).

Positive BODIPY was detected in liver sections using an IX71 Olympus Inverted Brightfield and Fluorescence Microscope (Hitschfel Instruments, Inc., St. Louis, MO) and images captured using Hamamatsu ORCA-ER digital camera and HCImage software. BODIPY was detected in placenta sections using a Nikon A1R-Ti2 confocal microscope, taking 1 µm z-stack projections at 60× magnification under oil. Three images were taken of each section moving from decidua to labyrinth (regions 1–3). Maximum intensity projections of the images were processed in Fiji and lipid droplet counts were determined using the Analyze Particles function of Fiji. Droplet counts were normalized using the ND female region 1 and therefore are reported as the average number of droplets in an experimental group per one droplet in the ND female region 1.

Serum extraction and mass spectrometry analysis

Lipids were extracted from serum using a modified Folch method. Briefly, 5 µL of serum was combined with PC 14:0/14:0 d54, an internal standard (Avanti Polar Lipids, Alabaster, AL). The combined solution was mixed with 70 µL of water, 100 µL of methanol, and 600 µL of chloroform. The solution was vortexed and centrifuged. The chloroform layer was collected, concentrated, and reconstituted in 50% methanol/water. This extracted sample was subsequently used to perform liquid chromatography—mass spectrometry (LC–MS).

The LC–MS was carried out using a Waters nanoAcquity fitted with a C18 BEH column and connected to a Waters Synapt G2-S mass spectrometer through an electrospray ionization source (Milford, MA). The mobile phase was water and methanol both

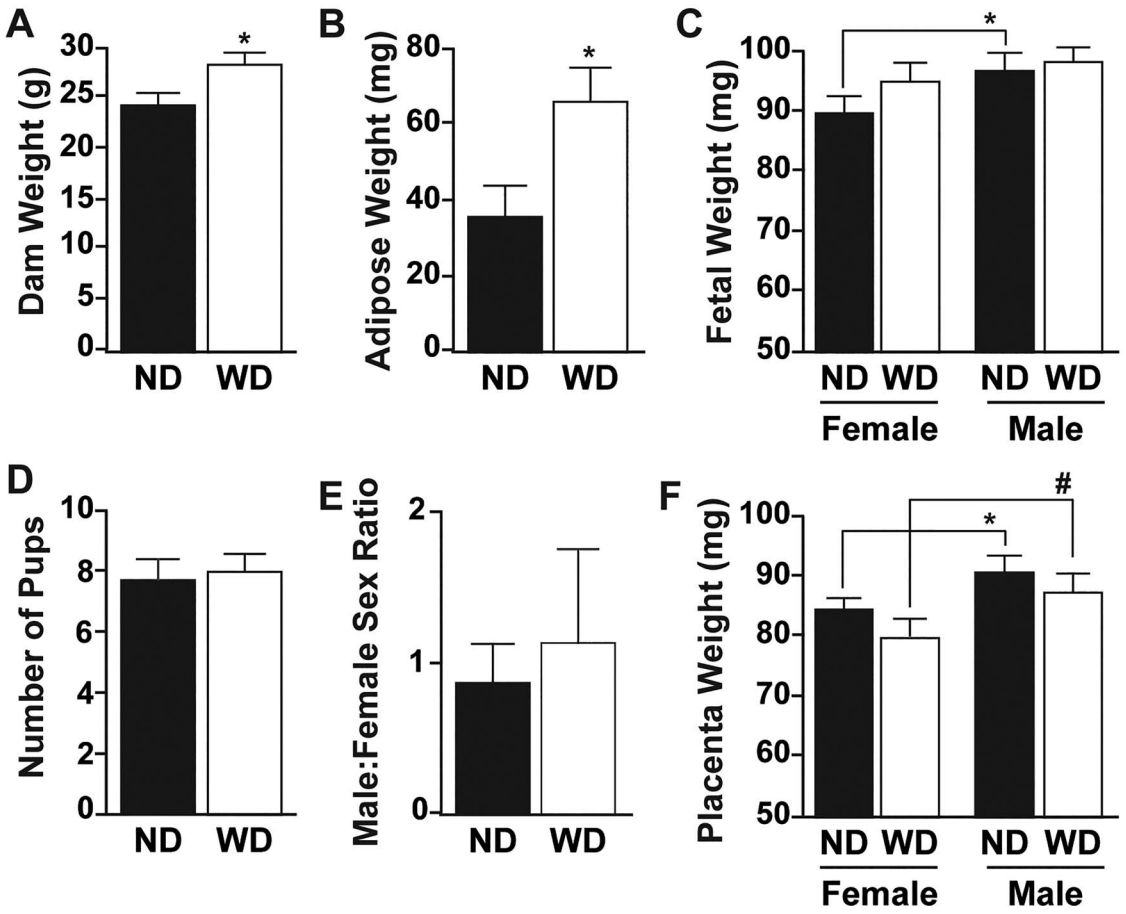

Figure 1. Body weight (A) and adipose tissue weights (B) of control (ND, n = 7) and western diet (WD, n = 5) dams. Fetal weights (C), were classified by dam diet (ND, WD) and fetal sex (F, female and M, male) at embryonic day 12.5 (ND-F n = 31, WD-F n = 23, ND-M n = 23, WD-M n = 17). Number of pups (D) and male-to-female sex ratio (E) in each experimental group (ND, n = 7 and WD, n = 5). (F) Placenta weights at embryonic day 12.5 classified by dam diet and fetal sex. All data are mean ± SEM, * $P < 0.05$, # $P < 0.1$.

with 50 µM of lithium acetate (Sigma Aldrich, St. Louis, MO). The capillary voltage and source temperature were maintained at 3.1 kV and 80°C, respectively. The data were analyzed using MassLynx 4.1 and DriftScope 2.7 (Waters). Putative lipid identifications were verified by MS/MS.

Mass spectrometry imaging

Placentas cryopreserved in OCT were sectioned (12 µm) and placed on Gold Seal Ultrastick glass slides (Thermo Fisher 3039). The slides were washed twice in HPLC grade water (1 min each) and dried in a vacuum desiccator. The matrix solution was 40 mg/mL of 2,5-dihydrobenzoic acid (DHB) in 70% methanol with 0.1% formic acid. Using an airbrush, matrix was sprayed onto the tissue section six times allowing the slide to dry between sprayings. Matrix assisted laser desorption/ionization (MALDI) based MS imaging was performed using a 15 Tesla Bruker SolariX XR mass spectrometer (Billerica, MA). The MALDI settings for number of laser shots and laser power were 1250 shots and 14%, respectively. After imaging, the slides were subjected to hematoxylin and eosin (H&E) staining to determine morphology. Briefly, slides were dried for 30 min at 37°C, washed in 70% ethanol for 1 min, placed in Mayer's Hematoxylin for 10 min, and then washed in ddH_2O for 2 min. Slides were subsequently dipped five times in Eosin Y and washed with ddH_2O to remove excess stain. Slides were dehydrated with sequential washes in 70%, 80%, 90%, and 100% ethanol and then incubated for 1 min in Citrisolv (Fisher). Slides were air dried and a coverslip applied using Permount. Images were obtained using an Olympus DP71 microscope and stitched together in Photoshop to generate an image of an entire placenta section. The H&E and MALDI images were overlayed to determine localization (labyrinth or decidua/junctional zone) of specific lipid species. MALDI images were processed using SCiLS (Bruker). Regions of interest were determined and outlined on H&E images and then applied to mass spectra images. Lipid identifications were assigned based on exact mass. Pearson's correlations were calculated using SCiLS which reported R-values of significant correlations ($P < 0.05$).

Droplet digital PCR

RNA was extracted from whole placenta and isolated labyrinth using Tri-reagent (Sigma) and reverse transcribed using Advanced iScript (Bio-Rad) per manufacturer instructions. Forward and reverse primers for mouse *Lpcat1*, *Lpcat2*, *Cept*, *Pcyt1a*, *Pla2g7*, *Elovl1*, *Fads1*, *Fads2*, *Pemt*, and *Actb* were designed using Primer-Blast (NCBI) and synthesized (Integrative DNA Technologies, Coralville, IA) (Supplementary Table 1). Positive control gBlocks

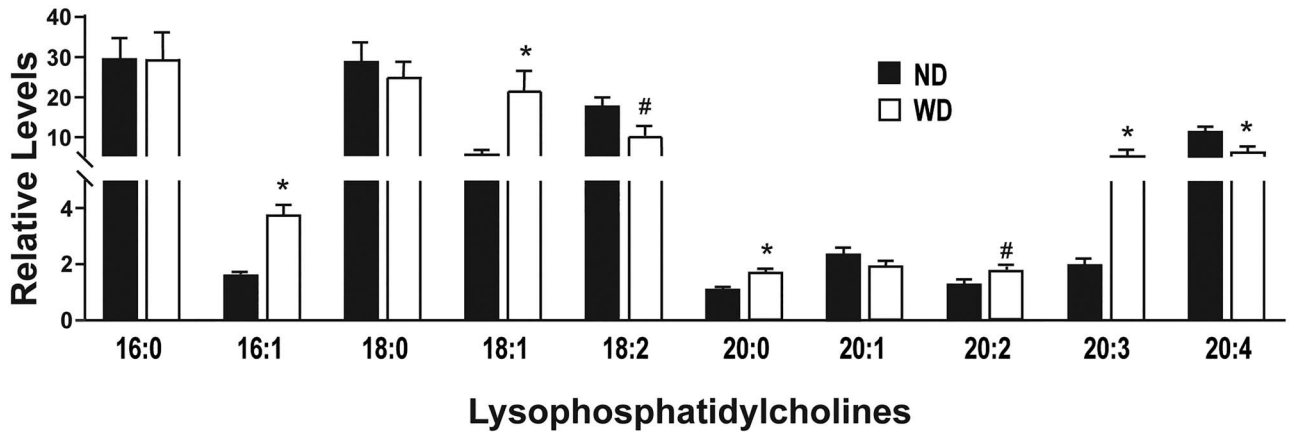

Figure 2. (A, B) Relative levels of serum lysophosphatidylcholines (LPC) between ND and WD dams (n = 3/experimental group). All data are mean ± SEM, $^{*}P < 0.05$, $^{\#}P < 0.1$.

Gene Fragments were designed based on the amplicon sequence for each gene and synthesized (Integrative DNA Technologies) (Supplementary Table 1).

Droplet digital PCR (ddPCR) was performed using the QX200 ddPCR BioRad system. Briefly, cDNA samples, gBlocks (positive control), or water (negative control) were combined with EvaGreen Supermix (Bio-Rad) and a gene-specific primer set. Droplets were generated (QX200 Droplet Generator) and PCR performed (C1000 Touch Thermal Cycler) using standard protocols. Fluorescence was detected using the droplet analyzer (QX200 Droplet Reader) and resulting positive and negative counts detected using QuantaSoft Analysis Pro. Copy number per microgram of cDNA was calculated for each transcript. The counts for *Lpcat1*, *Lpcat2*, *Cept*, *Pcyt1a*, *Pla2g7*, *Elovl1*, *Fads1*, *Fads2*, and, *Pemt* transcripts were normalized using counts of *Actb* for each sample. The stability of *Actb* across experimental groups was confirmed. Data are reported as gene copies per 10 000 copies of *Actb*.

nCounter gene expression assays

The multiplex nCounter gene expression assay was performed at the University of Nebraska Medical Center Genomics Core Facility using the pre-designed Mouse Metabolic Pathways Panel (Nanostring Technologies, Seattle WA). The panel includes 786 transcripts associated with biosynthesis and anabolic pathways, cell stress, nutrient transporter and catabolic pathways, metabolic signaling, and transcriptional regulation as well as 20 housekeeping genes.

The assay was performed according to the manufacturer's instructions. Briefly, total RNA collected from placental labyrinth was assessed for quality using the Agilent Bioanalyzer 2100. RNA (100 ng) was hybridized with proprietary capture and reporter probes. The RNA-probe complexes were purified, immobilized, and counted. Data were analyzed using the Advanced Analysis function in the nSolver Software 4.0 (Nanostring). Data were normalized using the *Tbp*, *Tlk2*, *Abcf1*, *Sdha*, *Ubb*, *Dhx16*, *Usp39*, *Agk*, *Fcf1*, and *Edc3* which were the most stable housekeeping genes present on the panel. Analysis covariates included dam diet, dam blood glucose, fetus weight, placental weight, and fetal sex.

Statistics

Body and adipose tissue weights of the dam, fetal weight, and placenta weight were analyzed in SAS (Cary, NC), using the PROC GLIMMIX analysis procedure. Fixed effects included dam treatment (ND or WD), fetal sex, and the interaction of fetal sex with dam treatment. The nested effect of dam within treatment was used as a random effect. Unpaired t-tests (GraphPad Prism 8) were used to analyze lipid levels in dam serum and ddPCR transcript abundance. One-way ANOVA was used to compare lipid levels between experimental groups in placenta sections. Paired t-test was used to compare lipid levels in the labyrinth and decidua/junctional zone within the same placenta. Two-way ANOVA with Sidak's multiple comparison test was used to compare placenta lipid droplet counts.

Results

Western diet increases dam adipose and body weight, has sex-specific effects on fetal weight

Dams were fed WD or ND prior to and during pregnancy until E12.5 as described in the materials and methods. As expected, WD dams had increased body and adipose tissue weight compared to ND counterparts (Figure 1A and B). However, there were no differences in total number of fetuses per litter (Figure 1D) or male-to-female fetus ratio (Figure 1E) between ND and WD dams. No differences in pregnancy failure were detected between experimental groups (data not shown). There was also no diet effect on E12.5 fetal weights. However, there was a difference between male and female fetal weights in the ND groups but not WD groups (Figure 1C). Similar to the fetal weight, there was no diet effect on placenta weight; however, there was a sex-dependent effect with male placentas heavier than female placentas (Figure 1F).

Western diet altered LPC profile in dam serum

Saturated and monounsaturated fatty acid content was higher and polyunsaturated fatty acid content lower in WD compared to ND. Palmitic acid (16:0) was 10-fold higher, stearic acid (18:0) was 25-fold higher, oleic acid (18:1 n9) was 4-fold higher, and linolenic acid (18:3 n3) was 2-fold higher in WD compared to ND. Conversely, linoleic acid (18:2 n6) was 4-fold lower in WD compared to ND. Based on the diet composition, we hypothesized that WD females would exhibit dyslipidemia.

Oxidative stress associated with obesity causes oxidation of circulating low-density lipoprotein (oxLDL), which significantly increases its LPC content [28]. Therefore, we measured circulating

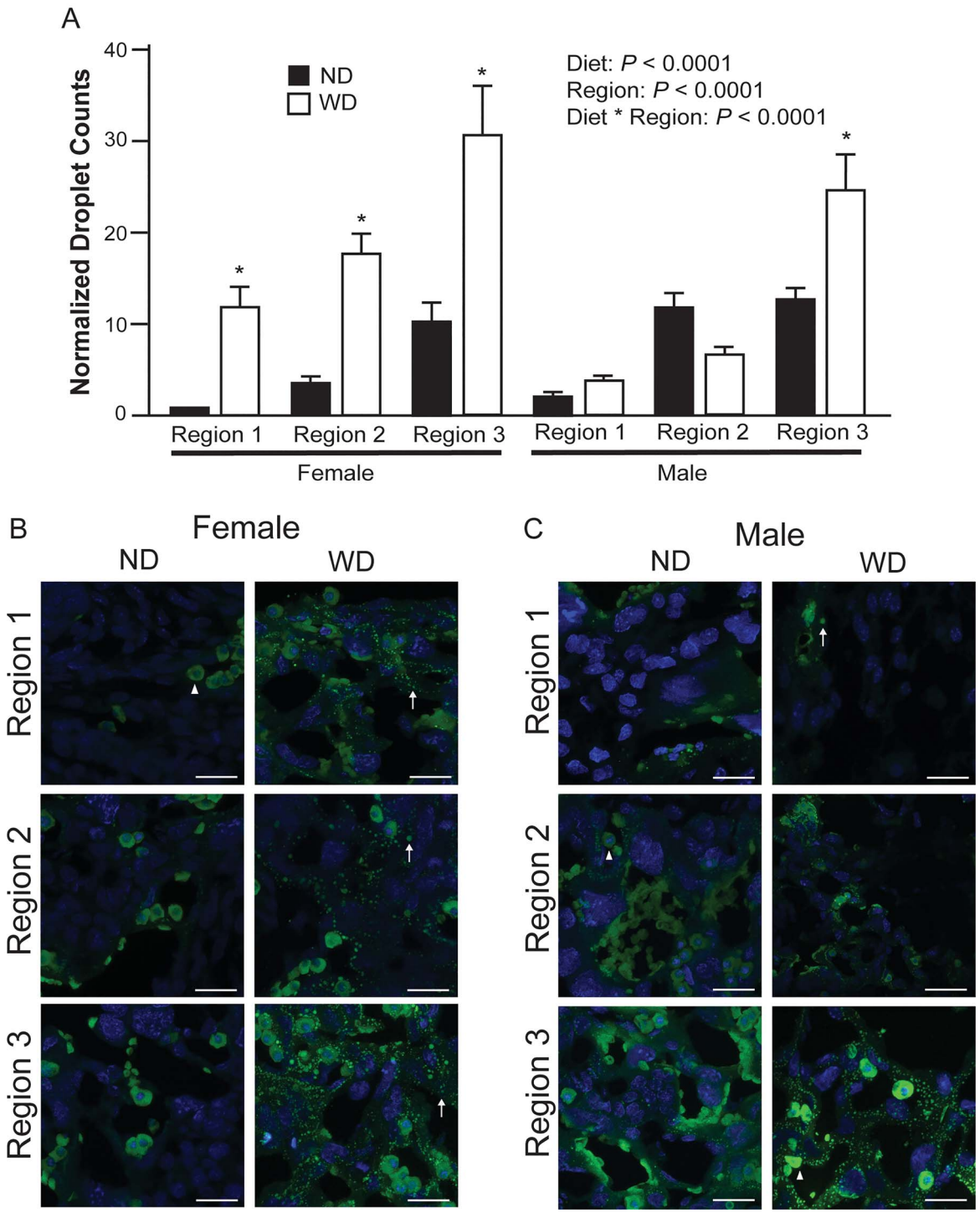

Figure 3. Droplet counts of BODIPY-stained placenta (A) from ND (n = 3 placentas/sex, 3 sections/placenta) and WD (n = 3 placentas/sex, 3 sections/placenta). Region 1 correlates with decidua, region 2 correlates with junctional zone, and region 3 correlates with labyrinth. Representative images from female (B) and male (C) placentas. Normalized droplet counts are the average number of droplets in each experimental group per one droplet in ND female region 1. Triangle indicates putative steroidogenic cell, arrow indicates a lipid droplet. Scale bars = 22 μm. All data are mean ± SEM, * indicates $P < 0.05$ for pairwise comparison of ND and WD.

LPC content in ND and WD dams as an indicator of dyslipidemia. LC–MS was performed using serum collected from ND (n = 3) and WD (n = 3) dams at euthanasia. Consistent with other studies [29, 30], the predominant circulating LPCs in lean and obese dams contained 16:0, 18:0, 18:1, 18:2, and 20:4 fatty acid tails (Figure 2). We also identified differences in the relative profiles of individual LPCs in WD compared to ND dams (Figure 2). Specifically, LPC containing 16:1 fatty acid was increased in WD compared to ND

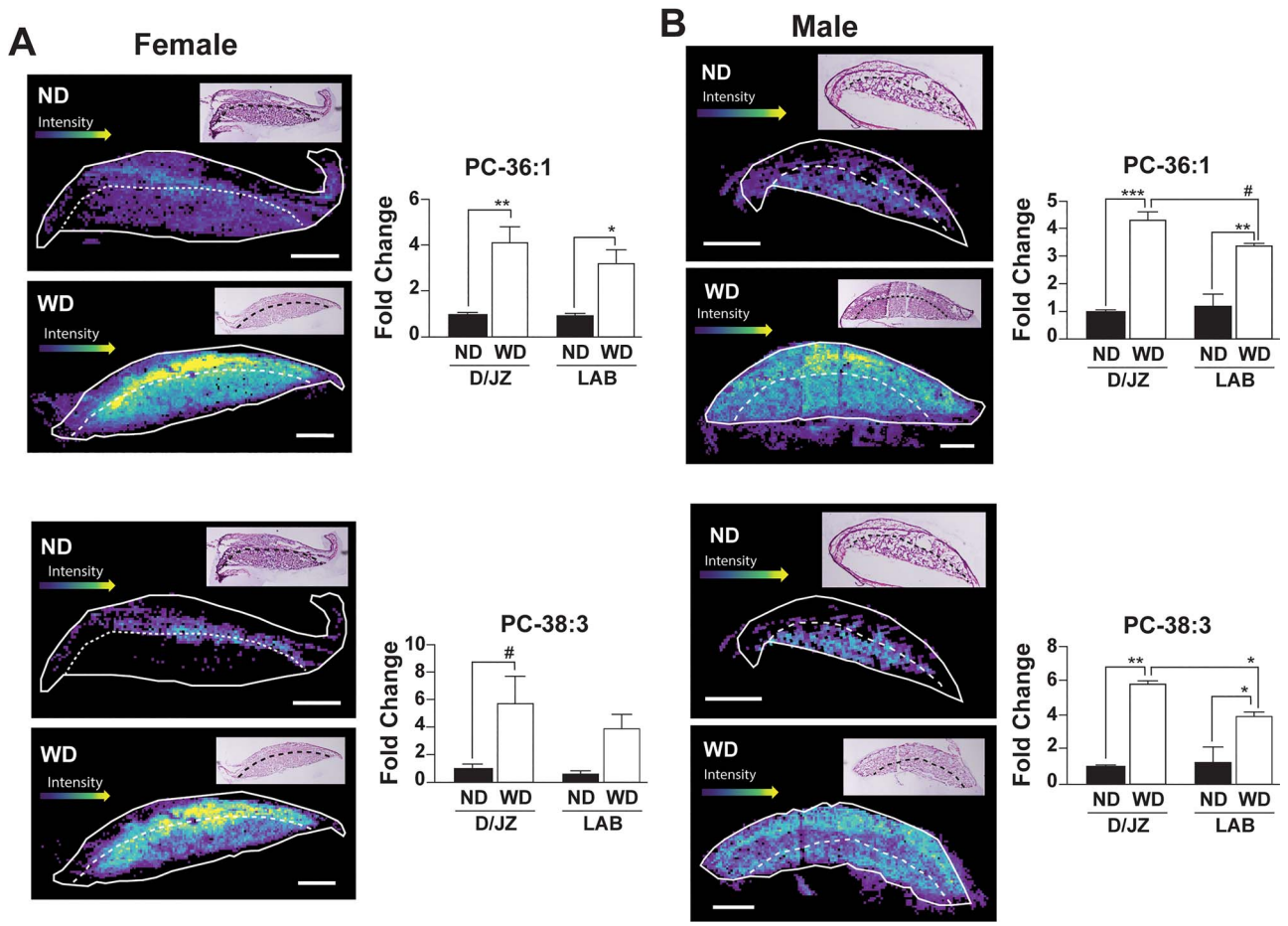

Figure 4. Representative images and relative quantification of PC 36:1 and PC 38:3, respectively in the labyrinth (LAB) and decidua/junctional zone (D/JZ) of male and female placentas (n = 3/experimental group). LAB and D/JZ are denoted by broken line based on tissue section morphology. Scale bar = 1 mm. All data are mean ± SEM, $^{****}P < 0.001$, $^{**}P < 0.01$, $^{*}P < 0.05$, $^{\#}P < 0.1$.

serum. However, there was no change in LPC containing a 16:0 fatty acid. There were more LPCs containing an 18:1 but no difference in 18:0-containing LPCs in WD compared to ND dam serum. Conversely, LPC 18:2 tended to be decreased in WD compared to ND serum. In 20-carbon LPCs, 20:0 and 20:3 were increased and 20:2 tended to be increased in WD serum, but 20:4 was decreased and 20:1 was unchanged compared to ND (Figure 2). In addition to the changes in circulating LPCs, lipid droplets, which were detected using the neutral lipid stain BODIPY, were increased in the WD compared to ND dam livers (Supplementary Figure 1).

The number of lipid droplets were increased in placentas from ND and WD dams

To determine if maternal dyslipidemia translated to altered placenta lipid content, we stained cryopreserved placentas from ND and WD dams with BODIPY. Sex-dependent differences in fetal responses to maternal obesity have been established [31–33]. Therefore, we classified placentas as male from a ND dam (n = 3), male from a WD dam (n = 3), female from a ND dam (n = 3), and female from a WD dam (n = 3) for these experiments. Confocal microscopy images of BODIPY-stained placenta were collected from regions of the placenta that corresponded to the decidua (1), junctional zone (2), and labyrinth (3). Using the Analyze Particles function of Fiji, increased lipid droplet counts ($P < 0.05$) were detected in regions 1 and 2 of WD compared to ND female placentas (Figure 3). However, there were no differences in lipid droplet counts between ND and WD male placentas in the same regions. Region 3, which is primarily the labyrinth of the placenta, had the highest content of lipids regardless of diet or sex. Lipid counts were also increased in WD compared to ND male and female placentas (Figure 3).

PCs 36:1 and 38:3 were increased in placentas from WD compared to ND dams

Lipid droplets are surrounded by a monolayer of phospholipids, which are predominately PCs [15]. Therefore, we hypothesized that there would be increased abundance and altered fatty acid composition of PCs in the male and female placentas from WD compared to ND dams. To test this hypothesis, we performed MS imaging, which allows spatially resolved MS data to be combined with tissue histology [34]. Thus, we not only determined relative abundance but also localization of specific lipid species in the labyrinth and junctional zone of the placenta.

Among the PCs with increased levels in placentas from WD dams were PC 36:1 and PC 38:3. There was a significant 3 to 4-fold increase in the relative abundance of PC 36:1 in male ($P < 0.001$, D/JZ and $P < 0.01$, LAB) and female ($P < 0.01$, D/JZ and $P < 0.05$, LAB) placentas collected from WD dams (Figure 4). Similar to PC 36:1, analysis of PC 38:3 showed increased abundance in the male

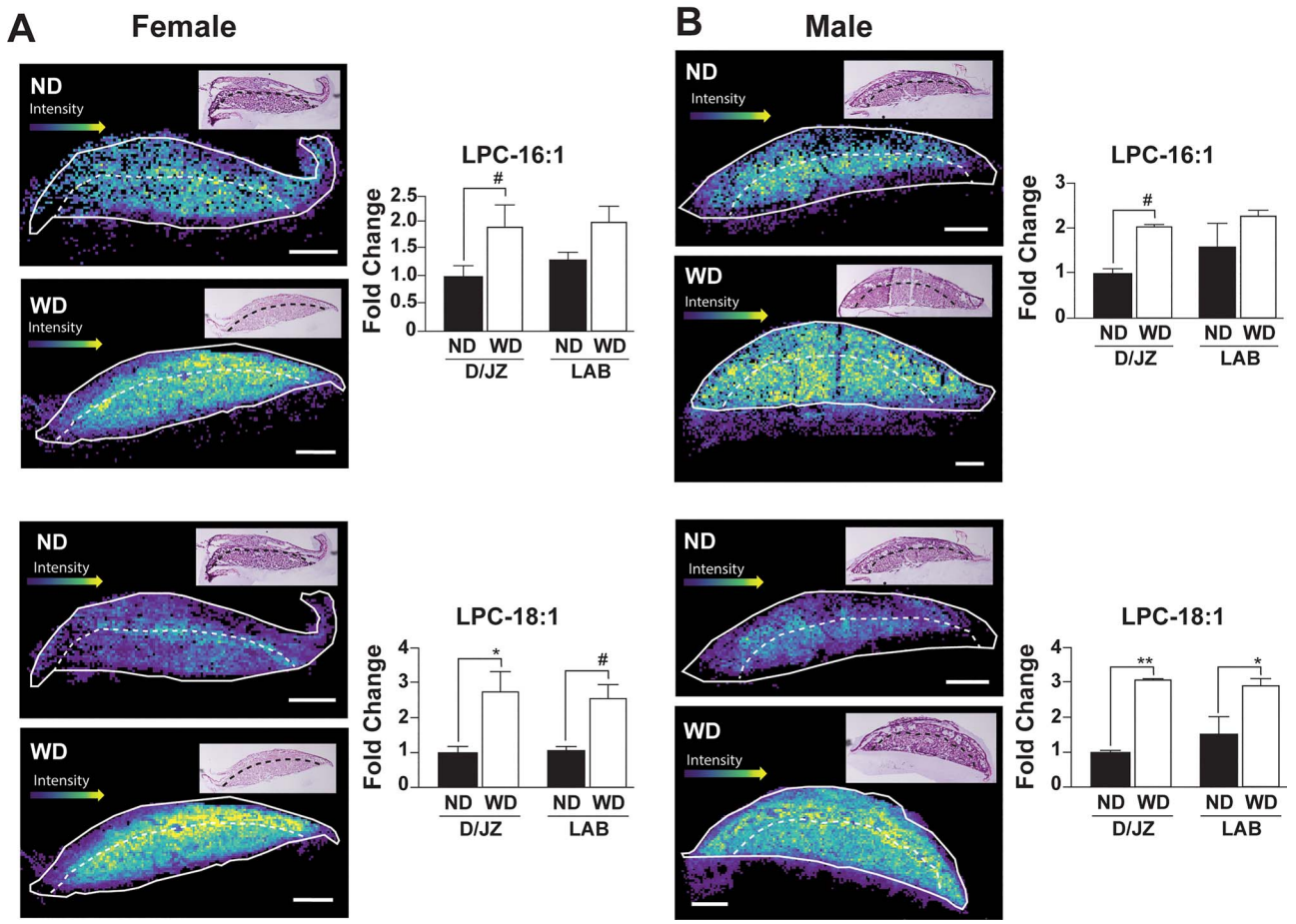

Figure 5. Representative images and relative quantification of LPC 16:1 and LPC 18:1, respectively in the labyrinth (LAB) and decidua/junctional zone (D/JZ) of female (A) and male (B) placentas (n = 3/experimental group). LAB and D/JZ are denoted by broken line based on tissue section morphology. Scale bars = 1 mm. All data are mean ± SEM, $^{**}P < 0.01$, $^{*}P < 0.05$, $^{\#}P < 0.1$.

placenta in both the D/JZ ($P < 0.01$) and LAB ($P < 0.05$) (Figure 4). However, in female placentas, PC 38:3 was not different in the LAB but tended to be increased in the D/JZ ($P < 0.1$) of placentas collected from WD dams (Figure 4).

Levels of 16-, 18-, and 20-carbon LPCs were increased in placentas from ND and WD dams

Increased phospholipase activity is associated with metabolically unhealthy, overweight individuals [35]. Therefore, we hypothesized that there would be increases in placental LPCs. Specifically, we measured LPC 16:1, 18:1, 20:1, and 20:3 which are potential lipase-dependent products of PC 36:1 and/or 38:3. There were no diet-dependent differences in LPC 16:1 in the labyrinth zone (LAB) in female or male placentas (Figure 5). Conversely, LPC 16:1 tended to be increased ($P < 0.1$) in the decidua/junctional zone (D/JZ) of both male and female placentas (Figure 5). The levels of LPC 18:1 were increased 3-fold ($P < 0.05$) in the D/JZ and LAB of both male and female placentas (Figure 5). When LPC 20:1 was analyzed in the D/JZ, it was increased 6-fold in male ($P < 0.05$) and female ($P < 0.1$) placentas. However, there was no difference in LPC 20:1 in the LAB of female and male placentas (Figure 6). There was also no difference in abundance of LPC 20:3 between ND or WD placentas in the LAB and D/JZ in from female fetuses. However, there was a 4 to 6-fold increase in 20:3 in both the LAB and D/JZ of male placentas (Figure 6).

Correlations between LPC and PC species in WD and ND derived placentas

To determine if the 16-, 18-, and 20-carbon LPCs were the result of phospholipase hydrolysis of PC 36:1 and/or PC 38:3, Pearson correlations were calculated between each of the LPCs and PCs in each experimental group (Table 1). There was a strong correlation (r = 0.6–0.79) between LPC 18:1 and PC 36:1 in female placentas and a moderate (r = 0.40–.059) to strong correlation in male placentas regardless of maternal diet (Table 1). There were also moderate to strong correlations between LPC 18:1 and PC 38:3 in both male and female placentas as well as strong (female) and moderate (male) correlations between PC 36:1 and PC 38:3. These data suggest that 18:1 fatty acid is one of the fatty acid tails in 36:1 and 38:3 PCs in biological membranes of the placenta. A strong correlation between LPC 16:1 and PC 36:1 in the LAB of ND male placentas was identified. However, there was no correlation between LPC 16:1 and PC 36:1 in the LAB of WD male placentas, D/JZ of ND and WD male placentas or either region of ND and WD female placentas (Table 1). There was also no correlation between LPC 16:1 and 38:3 in male or female placentas from ND dams. However, there was a modest correlation in the LAB and D/JZ of female WD

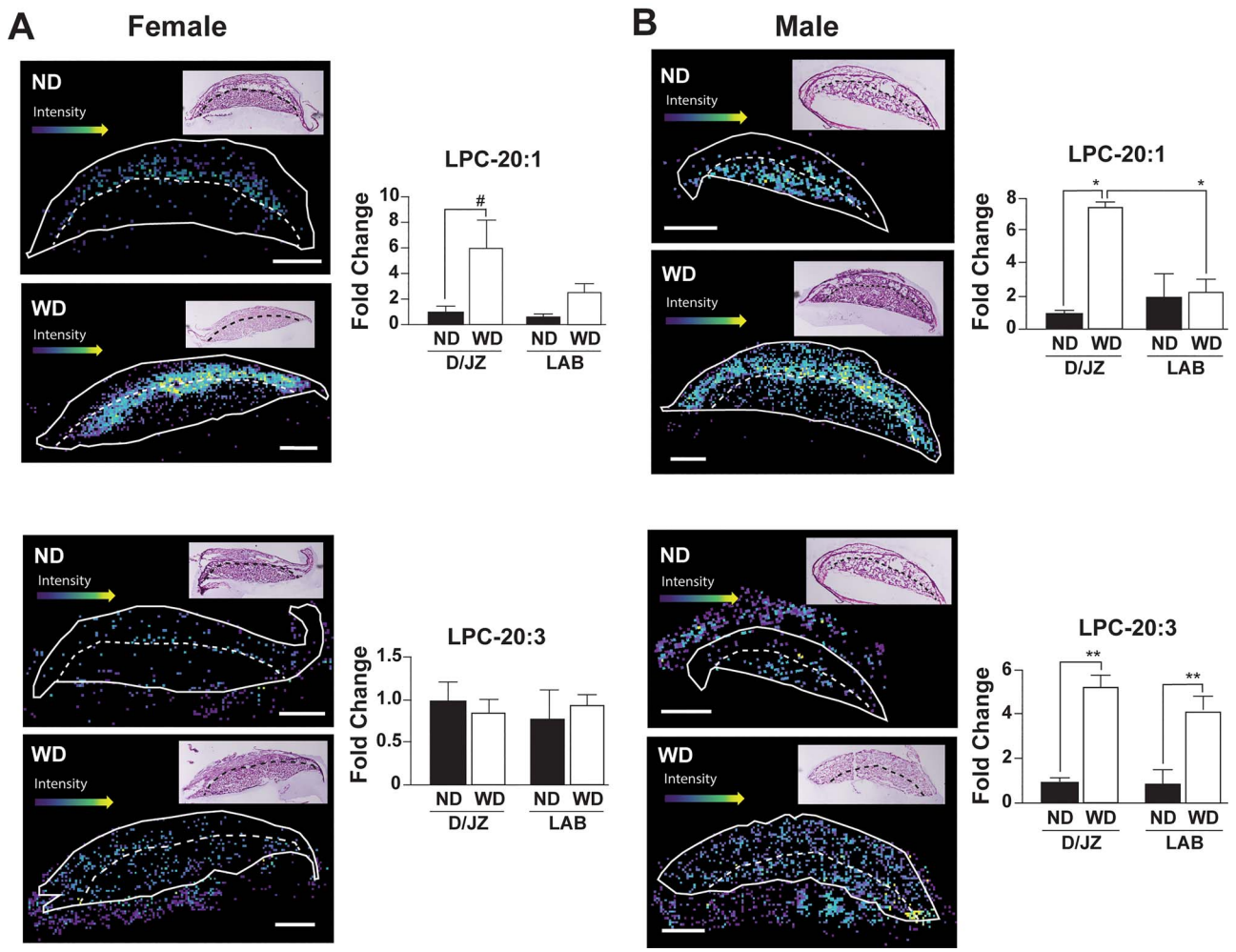

Figure 6. Representative images and relative quantification of LPC 20:1 and LPC 20:3, respectively in the labyrinth (LAB) and decidua/junctional zone (D/JZ) of female (A) and male (B) placentas (n = 3/experimental group). LAB and D/JZ are denoted by broken line based on tissue section morphology. Scale bar = 1 mm. All data are mean ± SEM, $^{**}P < 0.01$, $^{*}P < 0.05$, $^{\#}P < 0.1$.

placentas and in the LAB but not D/JZ of male WD placentas. These data suggest a potential effect of diet on the incorporation of 16:1 fatty acid into PC 38:3. There was no correlation between PC 36:1 or PC 38:3 and either of the 20-carbon LPCs. Interestingly, there was a moderate to strong correlation between LPC 16:1 and LPC 18:1 in both male and female placentas from ND and WD dams (Table 1).

Expression of genes associated with lipid metabolism in whole placenta and isolated labyrinth

To assess if placental PC and LPC differences were due to diet-dependent differences in the expression of lipid metabolism genes, ddPCR was performed. Specifically, genes involved in the Land's cycle (*Lpcat1*, *Lpcat2*, *Pla2g7*, *Pla2g5*), Kennedy cycle (*Cept*, *Pcyt1a)* and PE conversion to PC (*Pemt*) were examined using RNA from both whole placenta and labyrinth. Expression of fatty acid elongation (*Elovl1*) and desaturation (*Fads1*, *Fads2*) genes were also assessed in the labyrinth. No differences were detected in any of these genes between ND and WD placenta (Table 2). Therefore, we broadened our approach and interrogated the expression of 786 genes associated with lipid metabolism and transport in labyrinth from ND and WD placentas using the nCounter Mouse Metabolic Pathways Panel, which is a multiplex gene expression assay. We identified significant increases in *Apoe* (4-fold), *Apoa4* (15-fold), and *ApoB* (19-fold) in WD compared to ND labyrinth. There also tended to be an increase in *Apoam* (20-fold), *Apoa2* (8.5-fold), and *Apoa1* (12.7-fold). These genes encode for apolipoproteins, which are integral to lipid transport, and particularly cholesterol, via the formation of lipoproteins. However, there were no differences in any other genes associated with the transport of fatty acids or other nutrients (Table 2).

Discussion

One common characteristic of obesity is dyslipidemia [36] and increased lipid deposition in tissues which leads to lipotoxicity, inflammation, and oxidative stress [37]. In the current study, we identified increases in specific PC and LPC species in the placenta when mouse dams were fed a western diet (WD) compared to standard rodent chow (ND). Using MS imaging, we also identified spatial dependent differences in placenta PC and LPC, which to our knowledge has not been previously reported. This is also one of the first studies in the literature to demonstrate obesity-dependent differences in placental lipid content at E12.5 of gestation, which is

Table 1. Correlation coefficients between LPCs and PCs

Female Placenta			LPC16:1	LPC18:1	LPC20:1	LPC20:3	PC36:1	PC38:3
LPC 16:1	ND	D/JZ		**0.46**	0.10	0.03	0.30	0.33
		LAB		**0.44**	0.04	0.01	0.30	0.12
	WD	D/JZ		**0.68**	0.35	0.16	0.33	**0.47**
		LAB		**0.64**	0.07	0.13	0.55	**0.40**
LPC 18:1	ND	D/JZ	**0.46**		0.20	0.04	**0.62**	**0.68**
		LAB	**0.44**		0.12	0.03	**0.63**	**0.46**
	WD	D/JZ	**0.68**		**0.60**	0.31	**0.64**	**0.76**
		LAB	**0.64**		0.22	0.21	**0.76**	**0.69**
LPC 20:1	ND	D/JZ	0.10	0.20		0.02	0.12	0.18
		LAB	0.04	0.12		0.01	0.10	0.15
	WD	D/JZ	0.35	0.60		0.16	0.33	**0.47**
		LAB	0.07	0.22		0.07	0.13	0.27
LPC 20:3	ND	D/JZ	0.03	0.04	0.02		0.03	0.04
		LAB	0.01	0.03	0.01		0.02	0.06
	WD	D/JZ	0.16	0.31	0.16		0.30	0.35
		LAB	0.13	0.21	0.7		0.21	0.27
PC 36:1	ND	D/JZ	0.30	**0.62**	0.12	0.03		**0.60**
		LAB	0.30	**0.63**	0.10	0.02		**0.46**
	WD	D/JZ	0.33	**0.64**	0.33	0.30		**0.73**
		LAB	0.55	**0.76**	0.13	0.21		**0.75**
PC 38:3	ND	D/JZ	0.33	**0.68**	0.18	0.04	**0.60**	
		LAB	0.12	**0.46**	0.15	0.06	**0.46**	
	WD	D/JZ	**0.47**	**0.76**	**0.47**	0.35	**0.73**	
		LAB	**0.40**	**0.69**	0.27	0.27	**0.75**	
Male Placenta			LPC16:1	LPC18:1	LPC20:1	LPC20:3	PC36:1	PC38:3
LPC 16:1	ND	D/JZ		**0.48**	0.04	0.01	0.39	0.34
		LAB		**0.64**	0.12	0.04	**0.63**	0.30
	WD	D/JZ		**0.58**	0.21	0.07	0.33	**0.43**
		LAB		**0.48**	0.05	0.02	0.35	0.21
LPC 18:1	ND	D/JZ	**0.48**		0.13	0.02	**0.70**	**0.65**
		LAB	**0.64**		0.25	0.08	**0.83**	**0.64**
	WD	D/JZ	**0.58**		**0.42**	0.11	**0.46**	**0.69**
		LAB	**0.48**		0.16	0.04	**0.59**	**0.50**
LPC 20:1	ND	D/JZ	0.04	0.13		0.01	0.10	0.12
		LAB	0.12	0.25		0.05	0.21	0.36
	WD	D/JZ	0.21	0.42		0.05	0.17	0.34
		LAB	0.05	0.16		0.01	0.05	0.12
LPC 20:3	ND	D/JZ	0.01	0.02	0.01		0.01	0.03
		LAB	0.04	0.08	0.05		0.07	0.12
	WD	D/JZ	0.07	0.11	0.05		0.09	0.13
		LAB	0.02	0.04	0.01		0.02	0.09
PC 36:1	ND	D/JZ	0.39	**0.70**	0.10	0.01		**0.64**
		LAB	**0.63**	**0.83**	0.21	0.07		**0.54**
	WD	D/JZ	0.33	**0.46**	0.17	0.09		**0.58**
		LAB	0.35	**0.59**	0.05	0.02		**0.55**
PC 38:3	ND	D/JZ	0.34	**0.65**	0.12	0.03	**0.64**	
		LAB	0.30	**0.64**	0.36	0.12	**0.54**	
	WD	D/JZ	**0.43**	**0.69**	0.34	0.13	**0.58**	
		LAB	0.21	**0.50**	0.12	0.09	**0.55**	

Red bolded numbers represent a strong correlation (r = 0.6–0.79) and green bolded numbers represent moderate correlation (r = 0.40–0.59), n = 3 per each experimental group per each comparison.

Table 2. Gene expression in whole placenta and isolated labyrinth

ddPCR	Gene	ND	WD	*P*-value
Labyrinth	*Lpcat1*	43.41 ± 15.39	17.89 ± 6.22	0.16
	Lpcat2	10.02 ± 4.76	11.47 ± 1.91	0.91
	Cept	8.41 ± 3.57	6.45 ± 2.97	0.70
	Pcyt1a	38.83 ± 17.09	30.64 ± 8.35	0.67
	Pla2g7	125.70 ± 46.96	53.53 ± 16.23	0.22
	Elovl1	401.15 ± 114.58	202.95 ± 56.96	0.16
	Fads1	129.53 ± 52.33	88.43 ± 15.50	0.59
	Fads2	248.20 ± 98.8	112.00 ± 25.86	0.27
	Pemt	8.00 ± 2.03	4.66 ± 1.68	0.30
Whole Placenta	*Lpcat1*	82.78 ± 36.43	30.36 ± 16.3	0.23
	Lpcat2	13.04 ± 3.71	8.21 ± 3.00	0.36
	Cept	19.04 ± 6.322	8.07 ± 1.26	0.13
	Pcyt1a	4.63 ± 1.97	3.91 ± 0.85	0.75
	Pla2g5	1.59 ± 0.47	1.94 ± 0.53	0.64
	Pla2g7	126.33 ± 23.44	128.30 ± 13.05	0.94
nCounter	Gene	WD/ND	*P*-value	
Labyrinth	*Apoam*	20.00	0.06	
	Apoa2	8.58	0.08	
	Apoa1	12.70	0.09	
	Apoc2	7.76	0.26	
	Apoe	4.37	**0.01**	
	Apoa4	15.8	**0.04**	
	Apob	19.4	**0.05**	
	Slc6a12	1.24	0.66	
	Slc16a6	0.94	0.69	
	Slc1a5	1.04	1.00	
	Slc27a1	0.99	1.00	
	Slc3a2	1.07	0.24	
	Slc7a5	0.90	0.57	
	Acox1	1.17	0.04	
	Mcat	0.82	0.16	
	Slc25a1	1.20	0.42	
	Fabp5	0.91	0.78	
	Slc2a3	1.49	0.25	
	Slc2a1	0.98	0.91	

ddPCR, copies of target gene/10,000 copies Actb ± SEM normalized are shown in ND and WD samples nCounter, ratio of WD to ND counts (WD/ND) of representative genes from the nCounter Metabolism Panel.

the first day of a structurally and functionally mature placenta in the mouse.

LPCs are formed when a fatty acid tail (sn-1 or sn-2) is liberated from PCs in the cell membrane by phospholipase A2 (PLA2, cleaves at sn-2 position) [17], PCs in HDL by endothelial lipase (EL, cleaves at sn-1 position) [38], or by the oxidation of LDL which induces the activity of lipoprotein PLA2 (Lp-PLA2, cleaves at sn-2 position) [39]. We identified increased levels of LPCs containing 16:1, 18:1, 20:0, and 20:3 and decreased levels of LPCs containing 18:2, and 20:4 fatty acid tails in WD compared to ND dam circulation (Figure 2). We were unable to determine if the fatty acid was hydrolyzed at the sn-1 or sn-2 position. Nevertheless, Gauster et al. [40] demonstrated that EL activity preferentially generates LPC 18:2 and 20:4 from HDL. Furthermore, in vitro experiments by Orsó et al. [41] demonstrated that oxLDL by reactive oxygen species is enriched with saturated and monounsaturated LPC. Together, these data indicate that our WD dams acquired dyslipidemia.

A handful of studies have analyzed profiles of lipid classes in term placenta from women who were obese or lean prior to pregnancy. Increases in overall lipids, triglycerides, and non-esterified fatty acids have been reported [42–44]. Conversely, LC-PUFA and cholesterol esters were decreased in other studies [45, 46]. Uhl et al. [12] recently identified altered placental levels of PCs, PEs, and phosphatidylserines in obese and lean gestational diabetic compared to control women. Likewise, Chassen et al. [47] identified changes in the fatty acid composition of phospholipids in placentas from intrauterine growth restriction pregnancies. These collective studies did not measure and/or detect LPCs. However, a recent study by Gázquez et al. [48] demonstrated increased LPC 18:1 and PC 38:3 as well as overall increases in monounsaturated fatty acid containing LPCs in the lipid droplets of term placentas from obese compared to lean women. We similarly identified increases in LPC 16:1 (Figure 5), LPC 18:1 (Figure 5), LPC 20:1 (Figure 6), and PC 38:3 (Figure 4) in midgestation placentas from dams fed a WD suggesting that

alterations in placental lipid profiles develop at midgestation (or before) and are maintained throughout gestation.

In human term placentas from obese women, the mRNA abundance of *PLA2G2A* and *PLA2G5* are increased [49]. In this study, both *Pla2g7* and *Pla2g5* were expressed in placenta from ND and WD dams (Table 2), but we did not detect *Pla2g2a*. Furthermore, there was no diet-dependent difference in *Pla2g7* and *Pla2g5* expression. We did identify strong correlations between LPC 18:1/PC 36:1 and LPC 18:1/PC 38:3 (Table 1) in ND and WD male and female placentas. There was also a modest correlation between LPC 16:1/PC 38:3 in WD but not ND male and female placentas. Therefore, despite no differences in the expression of these enzymes, there may be increased phospholipase activity in the midgestation placenta. Furthermore, it is reasonable to infer that stearic acid (18:0), eicosadienoic acid (20:2, n6), and docosadienoic acid (22:2, n6) are increased as free fatty acids or esterified into triglycerides and stored in lipid droplets in WD placentas.

In human term placenta, fatty acid uptake by the syncytiotrophoblasts results in esterification and storage in lipid droplets in cytotrophoblasts [50]. Treatment of human term primary trophoblasts with linoleic and oleic acid increases their lipid droplets and cell viability [51]. Likewise, human term placentas collected from obese women exhibit increased palmitic acid (16:0) desaturation to palmitoleate (16:1), increased fatty acid esterification, and increased total lipids [10]. In the midgestation male and female placenta from WD dams, the number of lipid droplets were increased in the region of the labyrinth suggesting increased uptake of fatty acids from the maternal circulation (Figure 3). Interestingly, there were also increased lipid droplets in decidua and junctional zone regions of female but not male placentas. Increases in the number and size of lipid droplets necessitates synthesis of new phospholipids. We detected increased PC 36:1 and PC 38:3 in male and female placentas from WD dams (Figure 4). Synthesis of PCs is regulated by choline-phosphotransferase (CEPT) and choline-phosphate cytidylyltransferase (PCYT1A), which are enzymes in the de novo Kennedy cycle [52]. Alternatively, PC can be generated by conversion of PE to PC by PEMT or addition of a fatty acid to LPCs by lysophosphatidylcholine acyltransferase (LPCAT1, LPCAT2) [52]. Like the phospholipase genes, expression of *Cept, Pcyt1a, Pemt, Lpcat1*, *and Lpcat2* transcripts were not different between ND and WD whole placenta or isolated labyrinth (Table 2). However, Moessinger et al. [15] demonstrated that loss of LPCAT1 and LPCAT2 increases the size of lipid droplets. Thus, based on the increased number of lipid droplets as well as increased LPC content in the midgestation WD placenta, we hypothesize the activity of LPCAT1 and LPCAT2 was decreased in WD placentas.

Apolipoproteins are essential lipid binding proteins and major components of circulating lipoproteins (e.g., high-density lipoprotein, low-density lipoprotein). In the placenta, apolipoproteins play an important role in cholesterol efflux and therefore transport between the maternal and fetal circulation [53]. In placentas from WD dams, there were increases in several apolipoproteins (*Apoe, Apob, Apoa4*, $P < 0.05$ and *Apom, Apoa1, Apoa2*, $P < 0.1$; Table 2). Interestingly, Daniel et al. [54] demonstrated that protein restriction also increases *Apoa4, Apob*, and *Apoa2* in E13 rat placenta. We did not measure cholesterol in dam circulation, placenta, or fetus. However, the WD contained 0.2% cholesterol compared to no cholesterol in the ND. Therefore, the increases in apolipoprotein expression has the potential to increase fetal cholesterol at midgestation. Alternatively, Melhem et al. [55], showed that apoA1 and apoE are preferentially secreted by human term placenta to the maternal circulation. Thus, this preferential secretion may protect the fetus from excess accumulation of cholesterol.

In the term placenta, other studies have demonstrated obesity dependent increases in glucose, amino acid, and fatty acid transporters as well as genes associated with fatty acid β-oxidation [56–59]. However, we did not detect any diet-dependent changes in transporters or fatty acid binding proteins in the midgestation placenta (Table 2). This is consistent with the lack of weight differences between fetuses collected from ND and WD dams (Figure 1). Furthermore, we did not detect diet-dependent differences in PCs or LPCs in male and female fetuses (data not shown). Therefore, it is our conclusion that excess circulating maternal lipids are initially stored in lipid droplets particularly within the cytotrophoblasts of the E12.5 placenta. Once the capacity of the lipid droplets are reached, we would expect lipotoxicity to develop and subsequent compensatory changes in the placenta, which could lead to increased lipid transport at the end of gestation.

Supplementary material

Supplementary material is available at *BIOLRE* online.

Authors' contributions

KLB and ALR performed experiments, data analysis, and manuscript writing. ARM contributed to tissue collection and morphometric analyses. BDH wrote SAS code. EDD contributed to experimental design and manuscript edits, JRW managed the project including experimental design, data interpretation, and manuscript writing.

Acknowledgments

We thank Scott Kurz for assistance with animal care, Terri Fangman from the UNL Center for Biotechnology Microscopy Core (Nebraska Research Initiative) for assistance in confocal imaging, and the UNMC DNA Sequencing Core Facility.

Conflict of interest

The authors have declared that no conflict of interest exists.

References

1. Hales CM, Carroll MD, Fryar CD, Ogden CL. Prevalence of obesity among adults and youth: United States, 2015–2016. *Natl Cent Heal Stat* 2017; **1**:1–8.
2. Chiavaroli V, Castorani V, Guidone P, Derraik JGB, Liberati M, Chiarelli F, Mohn A. Incidence of infants born small- and large-for-gestational-age in an Italian cohort over a 20-year period and associated risk factors. *Ital J Pediatr* 2016; **42**:1–7.
3. Modi N, Murgasova D, Ruager-Martin R, Thomas EL, Hyde MJ, Gale C, Santhakumaran S, Doré CJ, Alavi A, Bell JD. The influence of maternal body mass index on infant adiposity and hepatic lipid content. *Pediatr Res* 2011; **70**:287–291.
4. Alfaradhi MZ, Ozanne SE. Developmental programming in response to maternal overnutrition. *Front Genet* 2011; **2**:1–13.
5. Gude NM, Roberts CT, Kalionis B, King RG. Growth and function of the normal human placenta. *Thromb Res* 2004; **114**:397–407.
6. Burton GJ, Fowden AL. The placenta: a multifaceted, transient organ. *Philos Trans R Soc B Biol Sci* 2015; **370**:20140066.
7. Carter AM. Evolution of placental function in mammals: the molecular basis of gas and nutrient transfer, hormone secretion, and immune responses. *Physiol Rev* 2012; **92**:1543–1576.

8. Myatt L, Maloyan A. Obesity and placental function. *Semin Reprod Med* 2016; **34**:42–49.
9. Kolahi KS, Valent AM, Thornburg KL. Cytotrophoblast, not syncytiotrophoblast, dominates glycolysis and oxidative phosphorylation in human term placenta. *Sci Rep* 2017; **7**:42941.
10. Calabuig-Navarro V, Haghiac M, Minium J, Glazebrook P, Ranasinghe GC, Hoppel C, De-Mouzon SH, Catalano P, O'Tierney-Ginn P. Effect of maternal obesity on placental lipid metabolism. *Endocrinology* 2017; **158**:2543–2555.
11. Gallo LA, Barrett HL, Dekker NM. Review: placental transport and metabolism of energy substrates in maternal obesity and diabetes. *Placenta* 2017; **54**:59–67.
12. Uhl O, Demmelmair H, Segura MT, Florido J, Rueda R, Campoy C, Koletzko B. Effects of obesity and gestational diabetes mellitus on placental phospholipids. *Diabetes Res Clin Pract* 2015; **109**:364–371.
13. Delhaes F, Giza SA, Koreman T, Eastabrook G, McKenzie CA, Bedell S, Regnault TRH, de Vrijer B. Altered maternal and placental lipid metabolism and fetal fat development in obesity: Current knowledge and advances in non-invasive assessment. *Placenta* 2018; **69**:118–124.
14. Tauchi-Sato K, Ozeki S, Houjou T, Taguchi R, Fujimoto T. The surface of lipid droplets is a phospholipid monolayer with a unique fatty acid composition. *J Biol Chem* 2002; **277**:44507–44512.
15. Moessinger C, Klizaite K, Steinhagen A, Philippou-Massier J, Shevchenko A, Hoch M, Ejsing CS, Thiele C. Two different pathways of phosphatidylcholine synthesis, the Kennedy pathway and the lands cycle, differentially regulate cellular triacylglycerol storage. *BMC Cell Biol* 2014; **15**:1–17.
16. Gibellini F, Smith TK. The Kennedy pathway—De novo synthesis of phosphatidylethanolamine and phosphatidylcholine. *IUBMB Life* 2010; **62**:414–428.
17. Law S-H, Chan M-L, Marathe GK, Parveen F, Chen C-H, Ke L-Y. An updated review of Lysophosphatidylcholine metabolism in human diseases. *Int J Mol Sci* 2019; **20**:1149.
18. Shindou H, Hishikawa D, Harayama T, Yuki K, Shimizu T. Recent progress on acyl CoA: lysophospholipid acyltransferase research. *J Lipid Res* 2009; **50**:S46–S51.
19. Huang YH, Schäfer-Elinder L, Wu R, Claesson HE, Frostegård J. Lysophosphatidylcholine (LPC) induces proinflammatory cytokines by a platelet-activating factor (PAF) receptor-dependent mechanism. *Clin Exp Immunol* 1999; **116**:326–331.
20. Treede I, Braun A, Sparla R, Kühnel M, Giese T, Turner JR, Anes E, Kulaksiz H, Füllekrug J, Stremmel W, Griffiths G, Ehehalt R. Anti-inflammatory effects of phosphatidylcholine. *J Biol Chem* 2007; **282**:27155–27164.
21. Cheng M, Pan H, Dai Y, Zhang J, Tong Y, Huang Y, Wang M, Huang H. Phosphatidylcholine regulates NF-κB activation in attenuation of LPS-induced inflammation: evidence from in vitro study. *Animal Cells Syst (Seoul)* 2018; **22**:7–14.
22. Jung YY, Nam Y, Park YS, Lee HS, Hong SA, Kim BK, Park ES, Chung YH, Jeong JH. Protective effect of phosphatidylcholine on lipopolysaccharide-induced acute inflammation in multiple organ injury. *Korean J Physiol Pharmacol* 2013; **17**:209–216.
23. Soncin F, Khater M, To C, Pizzo D, Farah O, Wakeland A, Rajan KAN, Nelson KK, Chang CW, Moretto-Zita M, Natale DR, Laurent LC et al. Comparative analysis of mouse and human placentae across gestation reveals species-specific regulators of placental development. *Development* 2018; **145**:dev156273.
24. Georgiades P, Ferguson-Smith AC, Burton GJ. Comparative developmental anatomy of the murine and human definitive placentae. *Placenta* 2002; **23**:3–19.
25. Soncin F, Natale D, Parast MM. Signaling pathways in mouse and human trophoblast differentiation: a comparative review. *Cell Mol Life Sci* 2015; **72**:1291–1302.
26. Gheorghe CP, Goyal R, Mittal A, Longo LD. Gene expression in the placenta: maternal stress and epigenetic responses. *Int J Dev Biol* 2009; **54**:507–523.
27. Qu D, McDonald A, Whiteley KJ, Bainbridge SA, Adamson SL. *Layer-Enriched Tissue Dissection of the Mouse Placenta in Late Gestation*. Amsterdam, Netherlands: Elsevier; 2014.
28. Levitan I, Volkov S, Subbaiah PV, Oxidized LDL. Diversity, patterns of recognition, and pathophysiology. *Antioxid Redox Signal* 2009; **13**:39–75.
29. Pang L-Q, Liang Q-L, Wang Y-M, Ping L, Luo G-A. Simultaneous determination and quantification of seven major phospholipid classes in human blood using normal-phase liquid chromatography coupled with electrospray mass spectrometry and the application in diabetes nephropathy. *J Chromatogr B* 2008; **869**:118–125.
30. Heimerl S, Fischer M, Baessler A, Liebisch G, Sigruener A, Wallner S, Schmitz G. Alterations of plasma lysophosphatidylcholine species in obesity and weight loss. *PLoS One* 2014; **9**:e111348.
31. Kim DW, Young SL, Grattan DR, Jasoni CL. Obesity during pregnancy disrupts placental morphology, cell proliferation, and inflammation in a sex-specific manner across gestation in the Mouse1. *Biol Reprod* 2014; **90**:1–11.
32. Evans LS, Myatt L. Sexual dimorphism in the effect of maternal obesity on antioxidant defense mechanisms in the human placenta. *Placenta* 2017; **51**:64–69.
33. Maliqueo M, Cruz G, Espina C, Contreras I, García M, Echiburú B, Crisosto N. Obesity during pregnancy affects sex steroid concentrations depending on fetal gender. *Int J Obes (Lond)* 2017; **41**: 1636–1645.
34. Cazares LH, Troyer DA, Wang B, Drake RR, John Semmes O. MALDI tissue imaging: from biomarker discovery to clinical applications. *Anal Bioanal Chem* 2011; **401**:17–27.
35. Kim M, Yoo HJ, Ko J, Lee JH. Metabolically unhealthy overweight individuals have high lysophosphatide levels, phospholipase activity, and oxidative stress. *Clin Nutr* 2020; **39**:1137–1145.
36. Franssen R, Monajemi H, Stroes ESG, Kastelein JJP. Obesity and dyslipidemia. *Med Clin North Am* 2011; **95**:893–902.
37. Guebre-Egziabher F, Alix PM, Koppe L, Pelletier CC, Kalbacher E, Fouque D, Soulage CO. Ectopic lipid accumulation: a potential cause for metabolic disturbances and a contributor to the alteration of kidney function. *Biochimie* 2013; **95**:1971–1979.
38. McCoy MG, Sun G-S, Marchadier D, Maugeais C, Glick JM, Rader DJ. Characterization of the lipolytic activity of endothelial lipase. *J Lipid Res* 2002; **43**:921–929.
39. Macphee CH, Moores KE, Boyd HF, Dhanak D, Ife RJ, Leach CA, Leake DS, Milliner KJ, Patterson RA, Suckling KE, Tew DG, Hickey DMB. Lipoprotein-associated phospholipase A2, platelet-activating factor acetylhydrolase, generates two bioactive products during the oxidation of low-density lipoprotein: use of a novel inhibitor. *Biochem J* 1999; **338**:479–487.
40. Gauster M, Rechberger G, Sovic A, Hörl G, Steyrer E, Sattler W, Frank S. Endothelial lipase releases saturated and unsaturated fatty acids of high density lipoprotein phosphatidylcholine. *J Lipid Res* 2005; **46**:1517–1525.
41. Orsó E, Matysik S, Grandl M, Liebisch G, Schmitz G. Human native, enzymatically modified and oxidized low density lipoproteins show different lipidomic pattern. *Biochim Biophys Acta Mol Cell Biol Lipids* 2015; **1851**:299–306.
42. Strakovsky RS, Pan Y-X. A decrease in DKK1, a WNT inhibitor, contributes to placental lipid accumulation in an obesity-prone rat Model1. *Biol Reprod* 2012; **86**:1–11.
43. Saben J, Lindsey F, Zhong Y, Thakali K, Badger TM, Andres A, Gomez-Acevedo H, Shankar K. Maternal obesity is associated with a lipotoxic placental environment. *Placenta* 2014; **35**: 171–177.
44. Hirschmugl B, Desoye G, Catalano P, Klymiuk I, Scharnagl H, Payr S, Kitzinger E, Schliefsteiner C, Lang U, Wadsack C, Hauguel-De Mouzon S. Maternal obesity modulates intracellular lipid turnover in the human term placenta. *Int J Obes (Lond)* 2017; **41**: 317–323.
45. Mazzucco MB, Higa R, Capobianco E, Kurtz M, Jawerbaum A, White V. Saturated fat-rich diet increases fetal lipids and modulates LPL and leptin receptor expression in rat placentas. *J Endocrinol* 2013; **217**: 303–315.

46. Fattuoni C, Mandò C, Palmas F, Anelli GM, Novielli C, Parejo Laudicina E, Savasi VM, Barberini L, Dessì A, Pintus R, Fanos V, Noto A et al. Preliminary metabolomics analysis of placenta in maternal obesity. *Placenta* 2018; **61**:89–95.
47. Chassen SS, Ferchaud-Roucher V, Gupta MB, Jansson T, Powell TL. Alterations in placental long chain polyunsaturated fatty acid metabolism in human intrauterine growth restriction. *Clin Sci* 2018; **132**:595–607.
48. Gázquez A, Uhl O, Ruíz-Palacios M, Gill C, Patel N, Koletzko B, Poston L, Larqué E. Placental lipid droplet composition: Effect of a lifestyle intervention (UPBEAT) in obese pregnant women. *Biochim Biophys Acta - Mol Cell Biol Lipids* 2018; **1863**:998–1005.
49. Varastehpour A, Radaelli T, Minium J, Ortega H, Herrera E, Catalano P, Hauguel-de Mouzon S. Activation of phospholipase A2 is associated with generation of placental lipid signals and Fetal obesity. *J Clin Endocrinol Metab* 2006; **91**:248–255.
50. Kolahi K, Louey S, Varlamov O, Thornburg K. Real-time tracking of BODIPY-C12 long-chain fatty acid in human term placenta reveals unique lipid dynamics in cytotrophoblast cells. *PLoS One* 2016; **11**:e0153522.
51. Bildirici I, Schaiff WT, Chen B, Morizane M, Oh S-Y, O'Brien M, Sonnenberg-Hirche C, Chu T, Barak Y, Nelson DM, Sadovsky Y. PLIN2 is essential for trophoblastic lipid droplet accumulation and cell survival during hypoxia. *Endocrinology* 2018; **159**:3937–3949.
52. Penno A, Hackenbroich G, Thiele C. Phospholipids and lipid droplets. *Biochim Biophys Acta Mol Cell Biol Lipids* 1831; **2013**:589–594.
53. Woollett LA. Review: Transport of maternal cholesterol to the fetal circulation. *Placenta* 2011; **32**:S218–S221.
54. Daniel Z, Swali A, Emes R, Langley-Evans SC. The effect of maternal undernutrition on the rat placental transcriptome: protein restriction upregulates cholesterol transport. *Genes Nutr* 2016; **11**:27.
55. Melhem H, Kallol S, Huang X, Lüthi M, Ontsouka CE, Keogh A, Stroka D, Thormann W, Schneider H, Albrecht C. Placental secretion of apolipoprotein A1 and E: the anti-atherogenic impact of the placenta. *Sci Rep* 2019; **9**:1–12.
56. Lager S, Ramirez VI, Gaccioli F, Jang B, Jansson T, Powell TL. Protein expression of fatty acid transporter 2 is polarized to the trophoblast basal plasma membrane and increased in placentas from overweight/obese women. *Placenta* 2016; **40**:60–66.
57. Segura MT, Demmelmair H, Krauss-Etschmann S, Nathan P, Dehmel S, Padilla MC, Rueda R, Koletzko B, Campoy C. Maternal BMI and gestational diabetes alter placental lipid transporters and fatty acid composition. *Placenta* 2017; **57**:144–151.
58. Dubé E, Gravel A, Martin C, Desparois G, Moussa I, Ethier-Chiasson M, Forest J-C, Giguère Y, Masse A, Lafond J. Modulation of fatty acid transport and metabolism by maternal obesity in the human full-term placenta1. *Biol Reprod* 2012; **87**:1–11.
59. Rosario FJ, Kanai Y, Powell TL, Jansson T. Increased placental nutrient transport in a novel mouse model of maternal obesity with fetal overgrowth. *Obesity* 2015; **23**:1663–1670.